

Quantum correlations and metrological advantage among Unruh-DeWitt detectors in de Sitter spacetime

Samira Elghaayda^{1,*}, Asad Ali^{2,†}, M. Y. Abd-Rabbou^{3,4,‡}, Mostafa Mansour^{1,§} and Saif Al-Kuwari^{2,¶}

¹*Laboratory of High Energy Physics and Condensed Matter, Department of Physics,
Faculty of Sciences of Ain Chock, Hassan II University,
P.O. Box 5366 Maarif, Casablanca 20100, Morocco.*

²*Qatar Center for Quantum Computing, College of Science and Engineering, Hamad Bin Khalifa University, Doha, Qatar*

³*School of Physics, University of Chinese Academy of Science,
Yuquan Road 19A, Beijing, 100049, China*

⁴*Mathematics Department, Faculty of Science, Al-Azhar University,
Nassr City 11884, Cairo, Egypt*

A long-standing debate on Gibbons-Hawking (GH) decoherence centers on its unclear thermal nature. In this work, we investigate the robustness of quantum Fisher information (QFI) and local quantum uncertainty (LQU) in the presence of GH decoherence, using free-falling Unruh-DeWitt (UDW) detectors in de Sitter spacetime (dS-ST). The UDW detectors interact with a massless scalar field in dS-ST and are modeled as open quantum systems, with the field acting as the environment for which we use a master equation to describe their evolution. Our analysis investigates the roles of energy spacing, GH temperature, initial state preparation, and various de Sitter-invariant vacuum sectors on the optimization of QFI and LQU. We find that the optimal values of QFI and LQU depend on the selected de Sitter-invariant vacuum sector and increase with larger energy spacing. Our findings reveal that QFI exhibits resilience to GH decoherence, maintaining a pronounced local peak across a wider range of parameters. This robustness can be further enhanced through strategic initial state preparation and increased energy spacing, resulting in a higher maximum QFI value even under significant environmental decoherence. Our results underscore the critical role of GH thermality in governing QFI and LQU, offering valuable insights for advances in relativistic quantum metrology (RQM).

I. INTRODUCTION

Quantum information in curved spacetime (CST) plays a vital role in exploring the interplay between quantum physics and gravity [1–6]. Although the abstract properties of quantum fields in CST, such as their entanglement [7–9], can be studied directly, operational approaches that involve observers and detectors have historically advanced theoretical insights [10, 11]. The Minkowski vacuum, for instance, exhibits long-range entanglement [12], which can be transferred to local inertial systems via standard quantum mechanical coupling mechanisms [13]. Variants of this concept include CST [14], thermal states [15], and accelerating detectors [16]. This work will focus on CST, particularly de sitter spacetime (dS-ST) [17–19], which is significant in cosmology. In CST, the definition of vacuum states is essential for analyzing vacuum fluctuations. In dS-ST, vacuum states fall into two categories: dS-invariant states and states that violate dS invariance [20]. The dS-invariant vacuum is widely regarded as the natural choice, as its role in dS-ST parallels that of the Minkowski vacuum in flat spacetime.

The Unruh-DeWitt (UDW) detector is a crucial tool

for probing quantum fields within specific spacetime geometries [10, 21]. This detector is a microscopic two-level system (qubit) that couples locally to fluctuating backgrounds. In dS-ST, a co-moving UDW detector detects radiation with a thermal spectrum defined by the temperature $T_{GH} = \frac{H}{2\pi}$, where H is the Hubble parameter [11]. This phenomenon, known as the GH effect, demonstrates universality in various quantum fields. For a massless scalar field [22], the infrared divergence of the propagator has negligible influence, leaving the detector's overall response largely unaffected. To explore the dynamic properties of quantum fields in CSTs [10], the open quantum systems framework has gained prominence [23, 24]. This approach has proven valuable in examining the behavior of UDW detectors in diverse spacetime backgrounds [25–27]. Within this framework, the UDW detector is modeled as a localized open quantum system, while the fluctuations of the background quantum field act as an environment that induces dissipation and dephasing.

In the framework of inflationary cosmology, quantum fluctuations are stretched during inflation, leading to anisotropies in the cosmic microwave background (CMB). The initial state during inflation is highly squeezed [28], and a Bell inequality test has been proposed to confirm the quantum mechanical origin of these primordial density fluctuations. Traditionally, these fluctuations are thought to arise from a Bunch-Davies vacuum (BDV) in the infinite past. However, this assumption has been questioned due to the inaccessibility of field modes below the Planck scale, Λ [29]. Consequently, in-

* samira.elghaayda@etu.univh2c.ma

† asad68826@hbku.edu.qa

‡ m.elmalky@azhar.edu.eg

§ mostafa.mansour.fsac@gmail.com

¶ smalkuari@hbku.edu.qa

flation models incorporating non-BD initial conditions, including alternatives like dS-invariant vacua [20, 30], initial scalar field entanglement [31], and correlated bubble universes [32], have attracted growing interest. A particularly intriguing feature of dS-ST is the existence of α -vacua, an infinite class of dS-invariant vacuum states parameterized by a complex variable α . These states, originally introduced decades ago [20, 30], recently received renewed attention despite ongoing debates about their ultraviolet behavior [33–37]. As viable candidates for non-BD initial conditions, α -vacua offer the potential for trans-Planckian modifications to the CMB [38–40]. Realizing this requires establishing a robust connection between the parameter α and the high-energy cutoff scale, Λ [41, 42].

In quantum estimation theory, a central challenge is estimating unobservable parameters in a labeled quantum system using measurement data [43, 44]. Enhancing the precision of these estimates and achieving the quantum accuracy limit are key objectives. Due to its practical relevance, the quantum Fisher information (QFI) has been explored from multiple perspectives, leading to significant progress. For instance, it has been used to establish a statistical generalization of the Heisenberg uncertainty principle [45]. The measurement of QFI with finite precision was demonstrated in [46], and its connections to quantum correlations (QCs) [47, 48] and quantum coherence [49] have been established.

Recently, there has been a growing interest in integrating quantum metrology and quantum information within relativistic frameworks, particularly in exploring quantum fields in CSTs [4, 50, 51]. Additionally, numerous studies have investigated the characteristics of QFI in non-inertial frames [52, 53]. By leveraging relativistic effects in quantum systems, it has shown that measurement precision can be greatly improved [54]. This emerging discipline, referred to as relativistic quantum metrology (RQM), seeks to identify the fundamental limits of measurement accuracy when quantum and relativistic effects are jointly considered. Significant relativistic phenomena explored in this field include the Unruh-Hawking effect [55, 56], the expansion rate of Robertson-Walker universes [57], and the properties of Schwarzschild spacetime [58].

A. Contribution

Working within the framework of detector-field interactions, we study a localized system of two UDW detectors in dS-ST. Assuming weak interaction with a bath of scalar fields, the system behaves like an open quantum system, experiencing environmental decoherence due to the thermal nature of dS-invariant vacua, such as the GH effect. In this paper, we evaluate the LQU and QFI at the final equilibrium state of the system and analyze how factors such as the detector's energy spacing, GH decoherence, the choice of initial state, and the selection of

α -vacua influence LQU and QFI. Our findings highlight the robustness and enhanced sensitivity of LQU and QFI, illustrating their potential to enhance quantum estimation techniques in practical applications.

B. Organization

The rest of the paper is structured as follows: Sec. II introduces the model, where two UDW detectors interact with a scalar field in a dS-ST background. The master equation in Lindblad form is solved to obtain the final equilibrium state. This section also examines fundamental concepts, including QFI and LQU for bipartite states. In Sec. III, we explore the dynamics of UDW in non-BD vacua, which depend on the initial state preparation of the detectors, the GH decoherence effect, and different choices of superselection sectors of α -vacua. Sec. IV presents our results, and Sec. V concludes the paper.

II. PRELIMINARIES

This section presents the essential concepts for defining QFI and LQU for a localized UDW in dS-ST. We begin by describing the dynamics of a bipartite UDW, governed by a Lindblad master equation. Next, we examine the definitions and properties of QFI and LQU for bipartite systems.

A. Markovian dynamics of UDW detectors

To proceed, we should first explore the Markovian evolution of an accelerating UDW detector interacting with a scalar field. This interaction can be modeled as an open quantum system weakly coupled to a heat bath. The total Hamiltonian of the system, which includes the UDW detectors and the environment, is given by

$$\mathcal{H} = \mathcal{H}_D + \mathcal{H}_\chi + \mathcal{H}_{int}, \quad (1)$$

Here, \mathcal{H}_D represents the Hamiltonian of two independent detectors in the common co-moving frame. The internal dynamics of each two-level detector is governed by a matrix 2×2 , and \mathcal{H}_D can be concisely expressed as [4, 5, 23, 27].

$$\mathcal{H}_D = \frac{\omega}{2} \left(\hat{s}_3^{(a)} \otimes \hat{s}_0^{(b)} + \hat{s}_0^{(a)} \otimes \hat{s}_3^{(b)} \right) \equiv \frac{\omega}{2} \Gamma_3, \quad (2)$$

where the symmetrized bipartite operators, $\Gamma_i = \hat{s}_i^{(a)} \otimes \hat{s}_0^{(b)} + \hat{s}_0^{(a)} \otimes \hat{s}_i^{(b)}$ are defined using Pauli matrices \hat{s}_i^k ($i = 1, 2, 3$), with superscript $m = \{a, b\}$ labeling distinct detectors, and ω is the energy spacing of the detectors. \mathcal{H}_χ is the Hamiltonian of free massless scalar fields $\chi(x)$ satisfying the Klein-Gordon equation $\square \chi(x) = 0$ in dS-ST, with covariant d'Alembertian operator $\square \equiv g^{\mu\nu} \nabla_\mu \nabla_\nu$

determined by the chosen coordinate system [23, 59]. \mathcal{H}_{int} describes the interaction between the system of two detectors and the scalar field, assumed to be in the form of electric dipole interaction

$$\mathcal{H}_{int} = \lambda \left[(\hat{s}_2^{(a)} \otimes \hat{s}_0^{(b)}) \chi(t, \mathbf{x}^{(a)}) + (\hat{s}_0^{(a)} \otimes \hat{s}_2^{(b)}) \chi(t, \mathbf{x}^{(b)}) \right], \quad (3)$$

where λ is a small dimensionless coupling constant. As we aim to study the dynamical evolution of detectors' density matrix $\eta_{ab}(t) = Tr_\chi[\eta_{tot}(t)]$, where t is the proper time of detectors' world-line, we assume that the initial density matrix of the total system is separable, i.e., $\eta_{tot}(0) = \eta_{ab}(0) \otimes |0\rangle\langle 0|$, where $|0\rangle$ is the vacuum state of field $\chi(x)$ and $\eta_{ab}(0)$ is the system's initial density matrix. The complete system, including UDW detectors and bath, constitutes a closed system. Therefore, the total density matrix evolves according to Von Neumann equation $i\dot{\eta}_{tot}(t) = [\mathcal{H}, \eta_{tot}(t)]$. However, in the weak coupling limit, the open Markovian dynamics of two UDW detector states $\eta_{ab}(t)$ can be extracted from $\eta_{tot}(t)$, by partial tracing over all environmental degrees of freedom (massless scalar field), that satisfies Kossakowski–Lindblad master equation [60, 61]

$$\frac{\partial \eta_{ab}(t)}{\partial t} = -i [\mathcal{H}_{eff}, \eta_{ab}(t)] + \mathcal{L} [\eta_{ab}(t)], \quad (4)$$

with

$$\mathcal{H}_{eff} = \mathcal{H}_D - \frac{i}{2} \sum_{m,n=1}^2 \Omega_{ij}^{(mn)} \hat{s}_i^{(m)} \hat{s}_j^{(n)}, \quad (5)$$

and

$$\mathcal{L} [\eta_{ab}] = \sum_{\substack{i,j=1,2,3 \\ k,l=a,b}} \frac{\Omega_{ij}^{(mn)}}{2} \left[2\hat{s}_j^{(k)} \eta_{ab} \hat{s}_i^{(l)} - \left\{ \hat{s}_i^{(k)} \hat{s}_j^{(l)}, \eta_{ab} \right\} \right], \quad (6)$$

represents the non-unitary evolution term produced by the coupling with external fields. The Kossakowski matrices $\Omega_{ij}^{(mn)}$ can be determined by the Fourier Transform of the following Wightman functions of the scalar field

$$Y^{(mn)}(t - t') = \langle 0 | \chi(t, x^{(m)}) \chi(t', x^{(n)}) | 0 \rangle, \quad (7)$$

and its Fourier Transform is given by

$$\mathcal{Y}^{(mn)}(\omega) = \int_{-\infty}^{+\infty} d\Delta t e^{i\omega\Delta t} Y^{(mn)}(\Delta t), \quad (8)$$

here, the superscript $m, n = \{a, b\}$ labeling distinct detectors. For two-detector system, one can easily find that $Y^{(aa)} = Y^{(bb)}$ and $Y^{(ab)} = Y^{(ba)}$, which lead to $\mathcal{Y}^{(aa)} = \mathcal{Y}^{(bb)} \equiv \mathcal{Y}_0$ and $\mathcal{Y}^{(ab)} = \mathcal{Y}^{(ba)}$.

The master equation (4) enables us to describe the asymptotic equilibrium states of detectors at large times, which are governed by the competition between environment dissipation in CST background and QC generated through the Markovian dynamics of detectors

[25, 62]. For two-detector system, the initial interatomic separation $L \equiv |\mathbf{x}^{(a)}, \mathbf{x}^{(b)}|$ is a control parameter of correlation generation, as Kossakowski matrices now become distance-dependent since in general $\mathcal{Y}^{(ab)} = \mathcal{Y}^{(ba)} \equiv \mathcal{Y}(\omega, L) = \mathcal{Y}_0(\omega) f(\omega, L)$ for two separated detectors [23, 63], where $f(\omega, L)$ is an even function of frequency ω . It is not surprising [64] that the correlation generation between detectors would be more effective for smaller L , and becomes impossible for an infinitely large separation. It was shown in [65] that a proper L always exists below which the generated correlation can persist asymptotically in final equilibrium states under environment dissipation. Therefore, we can concisely fix a small interatomic separation, and only be concerned about the influence of environment decoherence on the equilibrium states of detectors. In such a situation, all the Kossakowski matrices become equal $\Omega_{ij}^{(aa)} = \Omega_{ij}^{(bb)} = \Omega_{ij}^{(ab)} = \Omega_{ij}^{(ba)}$ [26], where

$$\Omega_{ij} = \kappa_+ \delta_{ij} - i\kappa_- \epsilon_{ijk} \delta_{3,k} + \tau \delta_{3,i} \delta_{3,j}, \quad (9)$$

with

$$\kappa_\pm = \frac{1}{2} (\mathcal{Y}_0(\omega) \pm \mathcal{Y}(-\omega)), \quad \tau = \mathcal{Y}_0(0) - \kappa_+. \quad (10)$$

After solving the master equation (4), the final reduced density matrix of two-detector at asymptotic equilibrium can be expressed in a Bloch form [25, 62]

$$\eta_{ab}(t) = \frac{1}{4} [\hat{s}_0^{(a)} \otimes \hat{s}_0^{(b)} + \sum_{j=1}^3 \rho_j \Gamma_j + \sum_{i,j=1}^3 \rho_{ij} \hat{s}_i^{(a)} \otimes \hat{s}_j^{(b)}], \quad (11)$$

where

$$\rho_j = -\frac{R}{3+T^2} (\tau + 3) \delta_{3,j}, \quad (12)$$

and

$$\rho_{ij} = \frac{1}{3+T^2} [T^2(\tau + 3) \delta_{3,i} \delta_{3,j} + (\tau - T^2) \delta_{ij}], \quad (13)$$

Here, the ratio $T = \frac{\kappa_-}{\kappa_+}$ is determined by the dynamics of the system. The final equilibrium state is also dependent on the choice of initial state by $\tau = \sum_{ii} \eta_{ii}(0)$ which is a constant of motion and satisfies $\tau \in [-3, 1]$ to keep $\eta_{ab}(0)$ positive.

B. QFI

Here, we will review the concept of QFI and its calculation based on the spectral decomposition of the density operator. We define QFI using a probe state represented by η_ν , where ν is an unobservable parameter. The QFI concerning ν can be formulated as [66]

$$\mathfrak{F}_\nu = Tr[L_\nu^2 \eta_\nu], \quad (14)$$

where the symmetric logarithmic derivative, denoted by L_ν , is defined through the equation $\partial_\nu \eta_\nu = \frac{1}{2}(L_\nu \eta_\nu + \eta_\nu L_\nu)$. By expressing the density operator as $\eta_\nu = \sum_i \mu_i |\psi_i\rangle \langle \psi_i|$, where μ_i are the eigenvalues and $|\psi_i\rangle$ are the corresponding eigenstates, an analytical solution for the QFI was obtained as shown in [67].

$$\mathfrak{F}_\nu = \sum_i \frac{(\mu'_i)^2}{\mu_i} + \sum_i \mu_i \mathfrak{F}_{\nu,i} - \sum_{i \neq j} \frac{8\mu_i \mu_j}{\mu_i + \mu_j} |\langle \psi'_i | \psi_j \rangle|^2, \quad (15)$$

with

$$\mu'_i = \partial_\nu \mu_i, \quad |\psi'_i\rangle = \partial_\nu |\psi_i\rangle, \quad \mathfrak{F}_{\nu,i} = 4(\langle \psi'_i | \psi_j \rangle - |\langle \psi'_i | \psi_i \rangle|^2). \quad (16)$$

It is evident that \mathfrak{F}_ν is solely dependent on the support set of η_ν and remains unaffected by eigenstates outside this support set. The first term in Eq. (17) depends only on the eigenvalues of η_ν and corresponds to the classical part, while the second and third term corresponds to the quantum part. Given the eigenstates outlined in (32), all the vectors $|\psi'_i\rangle = 0$. Therefore, the QFI is entirely driven by the classical contribution

$$\mathfrak{F}_\nu = \sum_i \frac{(\mu'_i)^2}{\mu_i}. \quad (17)$$

C. LQU

As a key measure in our analysis, we introduce LQU as the minimum skew information obtainable from a single local measurement. Let η_{ab} be the state of a bipartite system. Define $K_\Delta = K_\Delta^{(a)} \otimes \hat{s}_0^{(b)}$ as a local observable, where $K_\Delta^{(a)}$ is a Hermitian operator on subsystem (a) with spectrum Δ , and $\hat{s}_0^{(b)}$ is the identity operator acting on subsystem (b). We assume that Δ is non-degenerate, corresponding to maximally informative observables on subsystem (a). The LQU with respect to subsystem (a), optimized over all local observables on (a) with non-degenerate spectrum Δ , is expressed as [68, 69].

$$\mathfrak{L}(\eta_{ab}) \equiv \min_{K_\Delta} \Upsilon(\eta_{ab}, K_\Delta), \quad (18)$$

where the skew information is defined as [68, 70]

$$\Upsilon(\eta_{ab}, K_\Delta) = -\frac{1}{2} \text{Tr}([\sqrt{\eta_{ab}}, K_\Delta]^2), \quad (19)$$

Based on this Ref-[70], we summarize the key characteristics of skew information: it is nonnegative, equals zero if and only if the state and the observable commute, and is convex, meaning it decreases under classical mixing. If a local operator K_Δ exists such that $\Upsilon(\eta_{ab}, K_\Delta) = 0$, then the quantum system described by the state η_{ab} shows no QC between its two subsystems. For bipartite states the LQU is expressed as [69]

$$\mathfrak{L}(\eta_{ab}) = 1 - \max(\vartheta_{11}, \vartheta_{22}, \vartheta_{33}). \quad (20)$$

where $\vartheta_{i,i=1,2,3}$ are the eigenvalues of the 3×3 symmetric matrix denoted Π , whose entries are defined as follows

$$\left(\Pi \right)_{ij} \equiv \text{Tr} \left\{ \sqrt{\eta_{ab}} \left(\hat{s}_i^{(a)} \otimes \hat{s}_0^{(b)} \right) \sqrt{\eta_{ab}} \left(\hat{s}_j^{(a)} \otimes \hat{s}_0^{(b)} \right) \right\}, \quad (21)$$

The Pauli matrices acting on subsystem (a) are denoted by $\hat{s}_i^{(a)}$ ($i = x, y, z$).

III. QFI AND LQU IN NON-BD VACUA

The dS-ST represents the simplest solution of Einstein's field equations when a positive cosmological constant, Λ , is present. dS-ST is maximally symmetric, characterized by the isometry group $\text{SO}(4, 1)$ in four dimensions. Its importance arises from two primary aspects. Firstly, the observed accelerated expansion of our Universe strongly suggests that it is influenced by a small, positive Λ or an equivalent form of dark energy. Secondly, the remarkable uniformity and isotropy of the Universe on large scales, as observed in the CMB, imply that the early Universe likely underwent a phase of rapid accelerated expansion, commonly referred to as cosmic inflation for which we suggest the reader see the Ref-[71] for further details.

Our benchmark system consists of freely falling UDW detectors in dS-ST, which interact weakly with a coupled massless scalar field. We employ the global coordinate system (r, X, θ, ϕ) , where the detectors are co-moving with the expansion. The line element of dS-ST is given by

$$ds^2 = dr^2 - \frac{\cosh^2(Hr)}{H^2} [dX^2 + \sin^2 X (d\theta^2 + \sin^2 \theta d\phi^2)], \quad (22)$$

where the Hubble parameter H defines a positive cosmological constant $\Lambda = 3H^2$ and a radius of curvature $l = H^{-1}$. If the initial separation between detectors is much smaller than the radius of curvature, i.e., $L \ll l$, the resulting correlation at asymptotic equilibrium becomes independent of L . As a result, the detectors' final equilibrium states take the form given in Eqs. (11) and (12-13) (see Fig. 1).

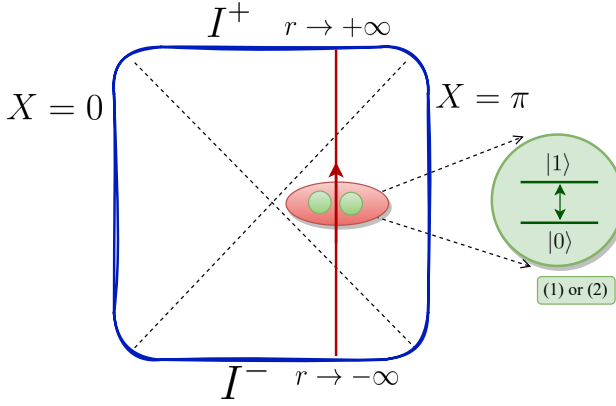


FIG. 1. Schematic illustration of the Penrose diagram for the global dS-ST is presented in the coordinates (22), where the two UDW detectors, labeled (1) and (2), follow geodesic trajectories in dS-ST with a small interatomic separation ($L \ll l$). The infinities, I^\pm , are space-like.

The scalar wave equation can then be resolved in coordinates (22), defining a dS-invariant BDV $|BD\rangle$. In the massless, conformal coupling limit, for a freely falling detector, the associated Wightman function $Y_{BD}^+(x(t), y(t')) \equiv \langle BD | \chi(x(t)) \chi(y(t')) | BD \rangle$ becomes [72]

$$Y_{BD}^+(x(t), y(t')) = -\frac{H^2}{16\pi^2 [(t - t')H/2 - i\epsilon]} \quad (23)$$

which fulfills Kubo-Martin-Schwinger (KMS) condition, i.e., $Y_{BD}^+(t') \equiv Y_{BD}^+(t' + i\beta)$, implying that for a detector in BDV sector, it ends up in thermal equilibrium at universal GH temperature $T_{GH} \equiv 1/\beta = 1/2\pi l$ [11].

By Mottola–Allen transformation, one can further define a one-parameter family of de Sitter-invariant vacua called α -vacua $|\alpha\rangle$, each of which can be interpreted as a squeezed state over $|BD\rangle$, i.e., $|\alpha\rangle = \hat{S}(\alpha) |BD\rangle$, where $Re\alpha < 0$ and $\hat{S}(\alpha)$ denotes a squeezing operator in quantum optics [33–37]. In particular, we adopt CPT invariant α -vacua, which means $\alpha < 0$ is real. Therefore, the Wightman function for the scalar field in α -vacua can be expressed in terms of Y_{BD}^+ as

$$Y_\alpha^+(x, y) = N^{-1} [Y_{BD}^+(x, y) + e^{2\alpha} Y_{BD}^+(y, x)] \quad (24)$$

where subscript α denotes a particular choice of α value, $N \equiv 1 - e^{2\alpha}$ and x_A is the antipodal point of x . As $\alpha \rightarrow -\infty$, we find that $Y_\alpha^+(x, y)$ reduces to the Wightman function in BDV $Y_{BD}^+(x, y)$, which uniquely extrapolates to the same short-distance behavior of two-point correlation function in the Minkowski vacuum, as the curvature of de Sitter vanishing. Employing the relation [73]

$$Y^+(x, y_A) = Y^+(x_A, y) = Y^+(t - i\pi), \quad (25)$$

and substituting (23) into (24), we can calculate the

Fourier transformation of the Wightman function in non-BD sectors as

$$\mathcal{Y} = \frac{\omega(1 + e^{\alpha - \pi\omega})^2}{2\pi(1 - e^{-\beta\omega})(1 - e^{2\alpha})}. \quad (26)$$

The related Kossakowski coefficients are

$$\begin{aligned} \Sigma_{+, \alpha} &= \frac{\omega [(1 + e^{\alpha - \pi\omega})^2 + e^{-\beta\omega}(1 + e^{\alpha + \pi\omega})^2]}{4\pi(1 - e^{-\beta\omega})(1 - e^{2\alpha})}, \\ \Sigma_{-, \alpha} &= \frac{\omega [(1 + e^{\alpha - \pi\omega})^2 - e^{-\beta\omega}(1 + e^{\alpha + \pi\omega})^2]}{4\pi(1 - e^{-\beta\omega})(1 - e^{2\alpha})}, \\ T_\alpha &= \frac{(1 + e^{\alpha - \pi\omega})^2 - e^{-\beta\omega}(1 + e^{\alpha + \pi\omega})^2}{(1 + e^{\alpha - \pi\omega})^2 + e^{-\beta\omega}(1 + e^{\alpha + \pi\omega})^2}. \end{aligned} \quad (27)$$

For fixed energy spacing of detectors, it is easy to find that $T_\alpha \in [-1, +1]$ as β varying. Inserting (27) into (11), we obtain the final equilibrium state of two detectors respecting to α -vacua, which is

$$\eta_{ab}(t) = \begin{pmatrix} \eta_- & 0 & 0 & 0 \\ 0 & \eta_{22} & \eta_{23} & 0 \\ 0 & \eta_{23} & \eta_{22} & 0 \\ 0 & 0 & 0 & \eta_+ \end{pmatrix}, \quad (28)$$

$$\eta_\pm = \frac{(3 + \tau)(T_\alpha \pm 1)^2}{4(3 + T_\alpha^2)}, \quad \eta_{23} = \frac{\tau - T_\alpha^2}{2(3 + T_\alpha^2)}, \quad (29)$$

$$\eta_{22} = \frac{3 - \tau - (1 + \tau)T_\alpha^2}{4(3 + T_\alpha^2)}. \quad (30)$$

The eigenvalues of the final state (28) are given by

$$\begin{aligned} \mu_1 &= \frac{(1 - T_\alpha)^2(\tau + 3)}{4(T_\alpha^2 + 3)}, & \mu_2 &= \frac{(T_\alpha + 1)^2(\tau + 3)}{4(T_\alpha^2 + 3)}, \\ \mu_3 &= \frac{(1 - T_\alpha^2)(\tau + 3)}{T_\alpha^2 + 3}, & \mu_4 &= \frac{1 - \tau}{4}. \end{aligned} \quad (31)$$

while the corresponding eigenvectors in the computational basis $\{|0\rangle, |1\rangle\}$ are

$$\begin{aligned} |\psi\rangle_1 &= |00\rangle, & |\psi\rangle_2 &= |11\rangle, \\ |\psi\rangle_3 &= \frac{1}{\sqrt{2}}(|10\rangle - |01\rangle), & |\psi\rangle_4 &= \frac{1}{\sqrt{2}}(|01\rangle - |10\rangle). \end{aligned} \quad (32)$$

Before proceeding to the QFI and LQU analysis of our model, it is necessary to consider several critical observations regarding α -vacua. First, the squeezing nature of α -vacua can significantly constrain measurement uncertainty, suggesting that certain intrinsic QCs may be concealed in these non-Bell diagonal states [74, 75]. Second, α -vacua does not exhibit thermal characteristics, as evidenced by the failure of (24) to satisfy the KMS condition unless it reduces to the BDV. This deviation from thermality has led to various attempts [38–40, 76] to consider α -vacua as an alternative initial state for inflation.

To account for the anticipated correction in the primordial power spectrum of order $\sim \mathcal{O}(H/\Lambda)^2$, the parameter α can be directly linked to Λ , which represents some fundamental scales of new physics (e.g., the Planck scale or the string scale) [41, 42].

We choose to estimate the GH parameter β for any arbitrary initial state. The related \mathfrak{F}_β can be straightforwardly calculated from (17), by substituting the eigenvalues (31) of the diagonalized density matrix of detectors system (28). According to different preparations of initial state encoded in $\tau \in [-3, 1]$, we come to two classes of QFI:

- (i) $\tau = -3$, only one nonvanishing eigenvalue $\mu_4 = 1$, which gives $\mathfrak{F}_\beta = 0$;
- (ii) $\tau \in (-3, 1]$, all eigenvalues (31) are non-vanishing. Since $\partial_\beta \mu_4 = 0$, we have

$$\mathfrak{F}_\beta = \sum_{i=1,2,3} \frac{(\mu'_i)^2}{\mu_i} = \frac{2(\tau+3)(R_\alpha^2-3)\partial_\beta R_\alpha^2}{(R_\alpha^2-1)(R_\alpha^2+3)^2}. \quad (33)$$

The explicit form of the matrix elements, which depend on the system parameters from (28) and the GH decoherence environment, is derived as

$$\vartheta_{11} = \vartheta_{22} = \frac{1}{4} (\sqrt{\eta_-} + \sqrt{\eta_+}) \times \left(\sqrt{1-\tau} + \sqrt{\frac{(1-R_\alpha^2)(\tau+3)}{R_\alpha^2+3}} \right), \quad (34)$$

and

$$\vartheta_{33} = \frac{\tau+3}{2} - \frac{(\tau+3)}{R_\alpha^2+3} + \sqrt{\frac{(1-\tau)(1-R_\alpha^2)(\tau+3)}{4(R_\alpha^2+3)}}, \quad (35)$$

while $\vartheta_{ij} = 0$ for $i \neq j$.

For $\tau \in [-3, 1]$, the situation for (33) and (34–35) is complicated due to its dependence on the infinite family

of non-BDV. In the following, our aim is to demonstrate that for certain initial states, QC can be generated in the final state (28) after the Markovian evolution of the system. To illustrate this, we consider two UDW detectors initially prepared in a Bell-diagonal state on a freely falling basis

$$\eta_{ab}(0) = \frac{1}{4} \left(\hat{s}_0^{(a)} \otimes \hat{s}_0^{(b)} + \sum_{i=1}^3 r_i \hat{s}_i^{(a)} \otimes \hat{s}_i^{(b)} \right), \quad (36)$$

with coefficients $0 \leq |r_i| \leq 1$. This state is the convex combination of four Bell states and reduce to maximally entangled states (Bell-basis) if $|r_1| = |r_2| = |r_3| = 1$.

IV. RESULTS AND ANALYSIS

In this section, we investigate the impact of GH decoherence on the QFI and LQU of scalar fields in dS-ST. To achieve this, we examined freely falling UDW detectors in dS-ST, which interact weakly with a massless scalar field in the dS-invariant BDV. This analysis allowed us to evaluate the degradation of QFI and LQU due to the GH effect, as a function of various physical parameters, including GH temperature $T_{GH} = 1/\beta$, the initial state preparation, α -vacua, and the detector energy spacing ω .

A. QFI

First, we evaluate how the QFI depends on various parameters to assess its effectiveness as a diagnostic tool for understanding the dS-ST structure. To illustrate our results, we will provide plots of QFI of GH versus the inverse of temperature β and different relevant system parameters, particularly the choice of the initial state, α -vacua, and the detector energy spacing.

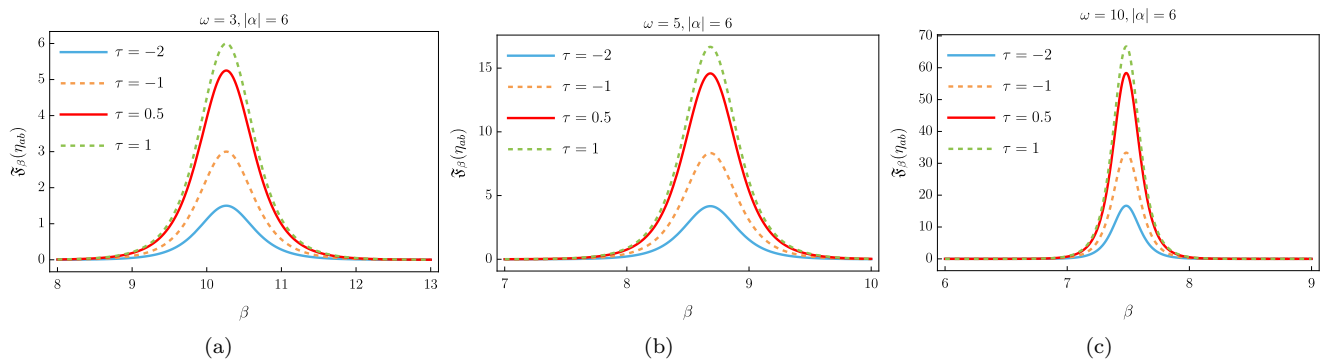


FIG. 2. The plot of QFI among UDW detectors as a function of β for various fixed values of τ , namely $\tau = -2$ (solid blue), $\tau = -1$ (dashed orange), $\tau = 0.5$ (solid red), and $\tau = 1$ (dashed green). In the left panel 2(a), we set $\omega = 3$ and $|\alpha| = 6$; in the middle panel 2(b), $\omega = 5$ and $|\alpha| = 6$; and in the right panel 2(c), $\omega = 10$ and $|\alpha| = 6$.

Figure 2 highlights intriguing features of the QFI as a function of the inverse GH temperature, β , and the initial state parameter, τ , with non-Bunch-Davies (non-BD) vacuum sectors fixed at $|\alpha| = 6$. QFI values are presented for fixed detector energy spacings $\omega = 3, 5, 10$. For all cases, a local peak emerges as β decreases, suggesting that optimal precision for estimating $\beta = 2\pi l$ is achieved with detectors at smaller curvature radii (l). QFI reaches a global maximum at an intermediate value β_{int} , after which it asymptotes to a smaller value. No-

tably, when $\tau < 0$ (e.g., $\tau = -2, -1$), QFI peaks are sharper, increasing and then rapidly decreasing around β_{int} . The location of β_{int} shifts with increasing ω , altering the QFI peak's position and amplifying the QFI, thereby lowering β_{int} in non-BD sectors. This indicates that optimal estimation for β depends significantly on the initial state choice. Additionally, as shown in Fig. 2(a), QFI initially rises to a maximum and then declines as β increases, while continuing to increase with τ . This trend underscores that higher precision in estimating β is achievable with an appropriate selection of τ .

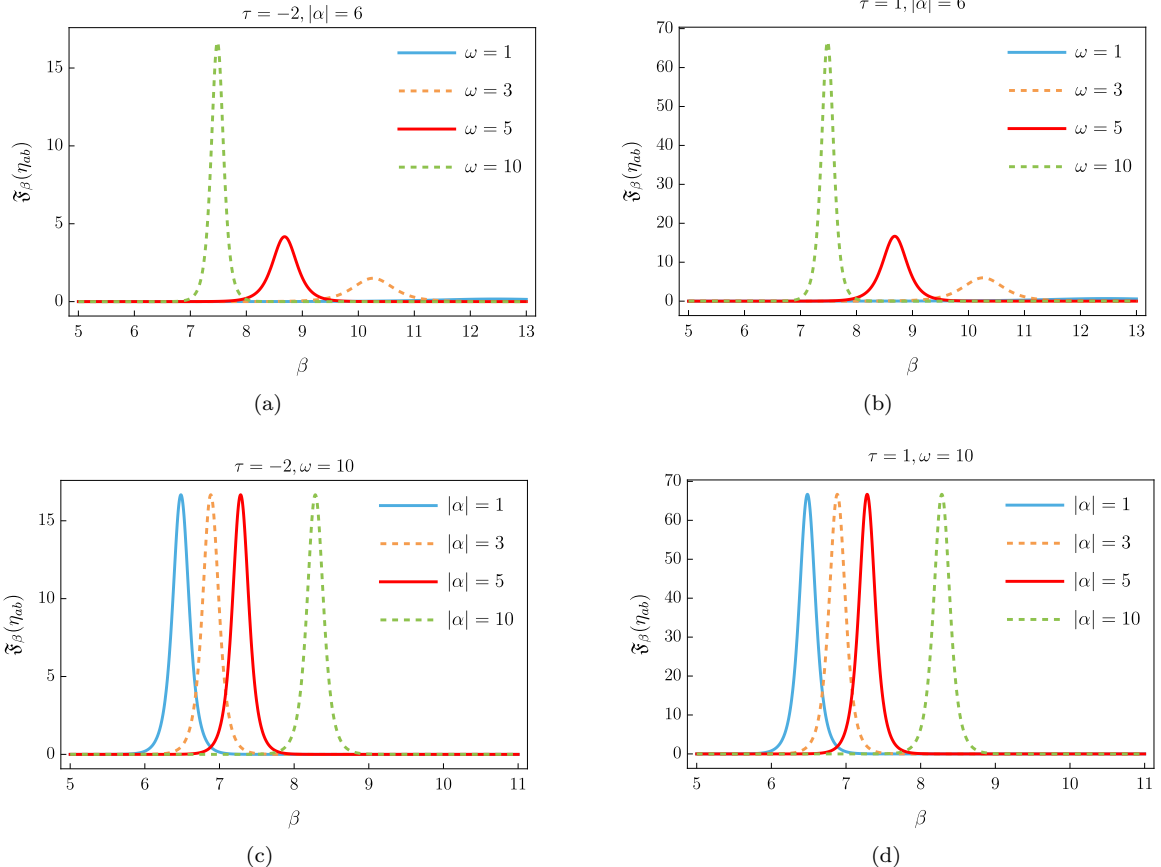


FIG. 3. The plots of QFI among UDW detectors as a function of β for various fixed parameters. Panels 3(a) and 3(b) depict QFI for different fixed values of ω , namely $\omega = 1$ (solid blue), $\omega = 3$ (dashed orange), $\omega = 5$ (solid red), and $\omega = 10$ (dashed green). In panel 3(a), we set $\tau = -2$ and $|\alpha| = 6$, while in panel 3(b), $\tau = 1$ and $|\alpha| = 6$. Panels 3(c) and 3(d) show QFI for different fixed values of $|\alpha|$, namely $|\alpha| = 1$ (solid blue), $|\alpha| = 3$ (dashed orange), $|\alpha| = 5$ (solid red), and $|\alpha| = 10$ (dashed green). In panel 3(c), we set $\tau = -2$ and $\omega = 10$, while in panel 3(d), $\tau = 1$ and $\omega = 10$.

Figure 3 presents the estimation degree of the GH coherence parameter, β , as determined by the QFI for various values of ω and $|\alpha|$. Figure 3(a) displays that increasing the energy spacing, ω , leads to an enhancement in the estimation precision of β . Additionally, a larger ω shifts the maximum bounds of the QFI towards lower values of β , which means higher precision of parameter

estimation can be achieved for the detector with a larger GH temperature. In line with the results presented in Fig. 2, increasing $\tau = 1$ results in a significant increase in the maximum QFI. Conversely, the impact of the coherence parameter, $|\alpha|$, on the QFI for β is explored in Fig. 3(c) and Fig. 3(d) for $\tau = -2$ and $\tau = 1$, respectively. The QFI exhibits a single peak that shifts towards

lower values of β as $|\alpha|$ increases. Notably, the maximum QFI remains relatively constant at approximately 15 for $\tau = -2$, while it significantly increases to around 70 for $\tau = 1$.

As evidenced in Fig. 2 and 3, a distinct Gaussian trend emerges. Examining the impact of various system parameters on QFI behavior, we observe that an augmentation in the value of τ results in an elevation of the maximum QFI value. This suggests that a higher τ enhances the system's quantum information processing capabilities. Increasing the value of $|\alpha|$ shifts the QFI maximum towards higher GH temperature values, while increasing ω shifts it towards lower GH temperature values. This indicates that the α -vacua and the detector energy spacing influence the probability distribution of quantum system interactions that contribute to enhancing the QFI. Physically, the ascending portion of the Gaussian curve signifies an increase in QFI with rising GH temperature values up to the inflection point. This implies that a higher GH

temperature value promotes quantum interactions that contribute to QFI growth, thereby strengthening quantum coherence among system components and improving quantum information processing capacity. Conversely, the descending portion of the curve, where QFI diminishes with increasing GH temperature, suggests that excessive GH temperature values may disrupt the system's quantum structure. This disruption can lead to the loss of quantum coherence, consequently diminishing the system's quantum information processing abilities.

B. LQU

Next, we demonstrate that the LQU arising from α -vacua can be harnessed as a resource in RQI tasks. We expect that the amount of LQU will exhibit dependence on the initial state preparation of the detectors and the various selections of superselection sectors of α -vacua.

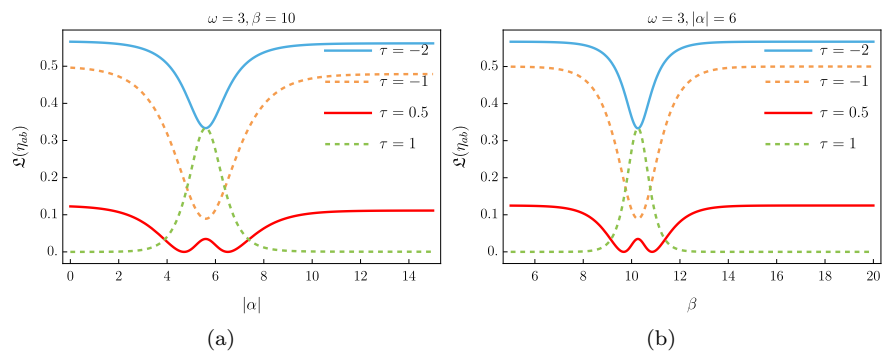


FIG. 4. The plots of LQU as a function of $|\alpha|$ (panel 4(a)) and β (panel 4(b)) for various fixed values of the parameter τ , namely $\tau = -2$ (solid blue), $\tau = -1$ (dashed orange), $\tau = 0.5$ (solid red), and $\tau = 1$ (dashed green). In both panels, $\omega = 3$, with $\beta = 10$ in 4(a) and $|\alpha| = 6$ in 4(b).

Figure 4 shows the QCs among two accelerated UDW detectors in dS-ST, evaluated using LQU for various initial state parameters τ and a fixed energy spacing of $\omega = 3$. Figure 4(a) plots the behavior of LQU as a function of $|\alpha|$ with a fixed $\beta = 10$. Negative values of τ yield higher levels of LQU compared to positive values. For negative τ , LQU gradually decreases with increasing $|\alpha|$. However, after reaching $|\alpha| > 5.5$, LQU begins to rise again, eventually reaching its maximum limit and evolving to different stable values for different initial states. Conversely, at $\tau = 1$, the system's LQU exhibits a single peak within the range $|\alpha| \in [4, 8]$. Outside this range, it remains zero, indicating a transition of the quantum system to a classical state. Similarly, Fig. 4(b) shows LQU

as a function of GH decoherence β with $|\alpha| = 6$. The system's behavior resembles that in Fig. 4(a), although the peak of LQU is shifted to $\beta \in [8, 12]$. These figures suggest that transitioning from negative to positive τ values can diminish LQU, indicating potential decoherence and a shift toward classical behavior. Additionally, the effects of $|\alpha|$ -vacua or β appear to similarly influence both the generation of LQU and its maximum limits. In particular, the decoherence environment has both positive and negative effects on LQU. Specifically, when the initial state is negative, the LQU increases with the GH effect. This result challenges the widespread belief that decoherence in the environment can only diminish LQU in dS-ST.

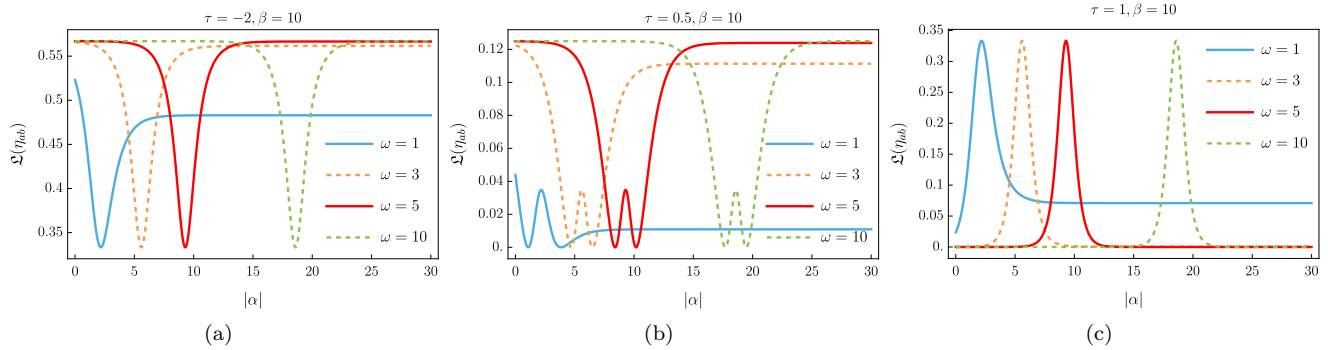


FIG. 5. The plot of LQU among UDW detectors as a function of $|\alpha|$ for various fixed values of ω , namely $\omega = 1$ (solid blue), $\omega = 3$ (dashed orange), $\omega = 5$ (solid red), and $\omega = 10$ (dashed green). In the left panel 5(a), we set $\tau = -2$ and $\beta = 10$; in the middle panel 5(b), $\tau = 0.5$ and $\beta = 10$; and in the right panel 5(c), $\tau = 1$ and $\beta = 10$.

The impact of varying values of ω and τ on LQU as a function of $|\alpha|$, with $\beta = 10$, is illustrated in Fig. 5. For $\tau = -2$ and different values of ω , Fig. 5(a) shows that lower ω values result in reduced LQU. However, as the energy spacing increases, the maximum LQU rises, peaking at 0.57. Additionally, there is a transient dip that shifts toward higher $|\alpha|$ values as ω increases. Conversely, Fig. 5(b) indicates that when $\tau = 0.5$, the maximum LQU values decrease. For lower ω values, the LQU approaches zero, which indicates that the system is nearing a clas-

sical state and experiencing increased decoherence. In contrast, Fig. 5(c) reveals that for $\tau = 1$, lower ω values yield higher LQU compared to higher ω values. As ω increases, there is still a shift in LQU toward higher $|\alpha|$ vacuum values. These results lead us to conclude that by jointly adjusting the energy spacing ω and the $|\alpha|$ vacuum for a specific choice of the initial state τ , we can significantly enhance the LQU of the system. This approach offers a viable solution to reduce the negative effects of the GH temperature on the two-detector system in CST.

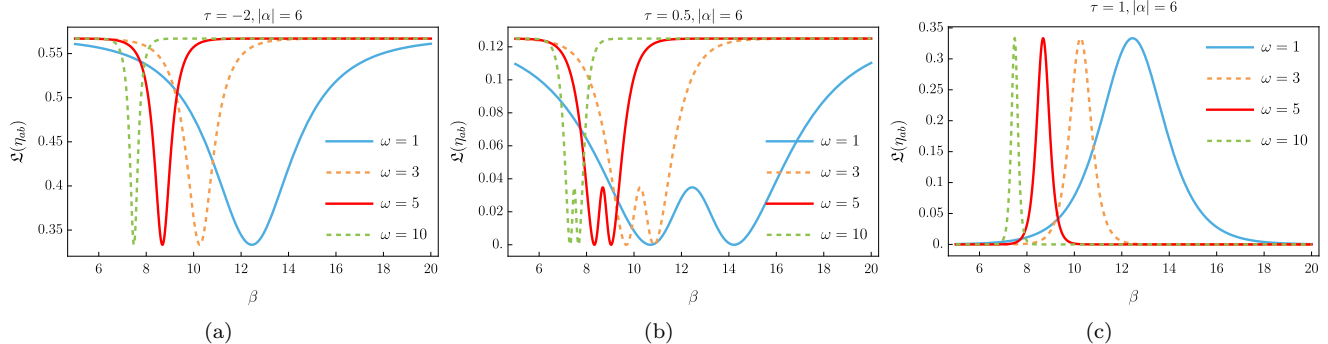


FIG. 6. The plot of LQU among UDW detectors as a function of β for various fixed values of ω , namely $\omega = 1$ (solid blue), $\omega = 3$ (dashed orange), $\omega = 5$ (solid red), and $\omega = 10$ (dashed green). In the left panel 6(a), we set $\tau = -2$ and $|\alpha| = 6$; in the middle panel 6(b), $\tau = 0.5$ and $|\alpha| = 6$; and in the right panel 6(c), $\tau = 1$ and $|\alpha| = 6$.

Now, we examine the impact of varying the values of ω and τ on the LQU as a function of the GH decoherence β with $|\alpha| = 6$. Figure 6 shows that, generally, an increase in ω enhances the LQU of the system, thus reducing decoherence. Specifically, Fig. 6(a) reveals a pit-like structure when $\tau = -2$; the width of this pit diminishes as the energy spacing increases and the bip shifts to lower β values. Conversely, positive values of τ influence the inversion of LQU. Figure 6(b) demonstrates

that the bip begins to broaden, and a small peak starts to form. However, when $\tau = 1$, Fig. 6(c) shows that the LQU is inverted, where the minimum bounds of LQU become the maximum bounds as τ increases. From this figure, it is evident that LQU represents a dynamic system significantly influenced by the control parameter τ . Continuous adjustments to τ induce topological transformations in the system's LQU. Initially, the function exhibits a concave (pit-like) profile, indicative of a stable

equilibrium point resembling a narrow well for large ω values. As τ transitions from negative to positive values, this well broadens, forming a small peak at the curve's center. This peak gradually intensifies until the function assumes a convex (peak-like) shape at $\tau = 1$. In this state, the peak represents the quantum region, while the remaining portion of the curve signifies the classical nature of the system.

V. CONCLUSION

In this paper, we investigated the thermal nature of the GH effect using QFI and LQU to evaluate the intrinsic estimation and correlations of non-BDV in dS-ST. We considered accelerating UDW detectors as open quantum systems coupled to massless scalar fields in the de Sitter-invariant vacuum, with the complete dynamics resolved from a Lindblad master equation for the density matrix.

As a result, we have observed the QFI of detectors can achieve the same maximum for different choices of de Sitter-invariant vacuum sectors, given fixed values of τ and ω . Moreover, the peak maximum of QFI can be enhanced by selecting appropriate energy spacing. However, GH decoherence generally reduces the QFI, which converges to an asymptotic value that is independent of the detector's initial state preparation. From a metrological perspective, this indicates that enhanced precision in estimating the GH effect can be achieved with relatively high energy spacing. Finally, we emphasize that when the initial state preparation is positive, specifically for

$\tau = 1$, the related QFI is robust against GH decoherence, in the sense that its local peak can persist over a very long range. This robustness of QFI can significantly facilitate practical relativistic quantum estimation tasks. Similarly, in our LQU analysis, we found that LQU exhibits a striking revival phenomenon as the GH temperature increases. In particular, the amount of LQU can drastically improve after a certain turning point, β_c , for non-BD sectors, due to the competition between GH decoherence and the intrinsic correlation of α -vacua. For certain choices of the detectors' initial state, the measure of LQU will first decrease to zero, then increase, and eventually approach an asymptotic value. Notably, LQU in specific non-BD sectors can persist even under arbitrarily large GH decoherence.

DISCLOSURES

The authors declare that they have no known competing financial interests.

DATA AVAILABILITY

No datasets were generated or analyzed during the current study.

ACKNOWLEDGMENTS

M.Y. Abd-Rabbou was supported in part by the University of Chinese Academy of Sciences.

[1] Jacob D Bekenstein. Black holes and entropy. *Physical Review D*, 7(8):2333, 1973.

[2] Matthew C Palmer, Maki Takahashi, and Hans F Westman. Localized qubits in curved spacetimes. *Annals of physics*, 327(4):1078–1131, 2012.

[3] Jacob D Bekenstein. Quantum information and quantum black holes. In *Advances in the Interplay Between Quantum and Gravity Physics*, pages 1–26. Springer, 2002.

[4] Samira Elghaayda, Xiang Zhou, and Mostafa Mansour. Distribution of distance-based quantum resources outside a radiating schwarzschild black hole. *Classical and Quantum Gravity*, 41(19):195010, 2024.

[5] Samira Elghaayda and Mostafa Mansour. Entropy disorder and quantum correlations in two unruh-dewitt detectors uniformly accelerating and interacting with a massless scalar field. *Physica Scripta*, 98(9):095254, 2023.

[6] Samira Elghaayda, MY Abd-Rabbou, and Mostafa Mansour. Quantum obesity and steering ellipsoids for fermionic fields in garfinkle-horowitz-strominger dilation spacetime. *arXiv preprint arXiv:2408.06869*, 2024.

[7] Stephen Hawking, Juan Maldacena, and Andrew Strominger. Dsitter entropy, quantum entanglement and ads/cft. *Journal of High Energy Physics*, 2001(05):001, 2001.

[8] Jonathan L Ball, Ivette Fuentes-Schuller, and Frederic P Schuller. Entanglement in an expanding spacetime. *Physics Letters A*, 359(6):550–554, 2006.

[9] Asad Ali, Saif Al-Kuwari, Mehrdad Ghominejad, MT Rahim, Dong Wang, and Saeed Haddadi. Quantum characteristics near event horizons. *Physical Review D*, 110(6):064001, 2024.

[10] Nicholas David Birrell and Paul Charles William Davies. Quantum fields in curved space. 1984.

[11] Gary W Gibbons and Stephen W Hawking. Cosmological event horizons, thermodynamics, and particle creation. *Physical Review D*, 15(10):2738, 1977.

[12] Stephen J Summers and Reinhard Werner. Maximal violation of bell's inequalities is generic in quantum field theory. *Communications in Mathematical Physics*, 110:247–259, 1987.

[13] Benni Reznik, Alex Retzker, and Jonathan Silman. Violating bell's inequalities in vacuum. *Physical Review A—Atomic, Molecular, and Optical Physics*, 71(4):042104, 2005.

[14] Eduardo Martin-Martinez and Nicolas C Menicucci. Entanglement in curved spacetimes and cosmology. *Classical and Quantum Gravity*, 31(21):214001, 2014.

[15] Daniel Braun. Entanglement from thermal blackbody radiation. *Physical Review A—Atomic, Molecular, and*

Optical Physics, 72(6):062324, 2005.

[16] Serge Massar and Philippe Spindel. Einstein-podolsky-rosen correlations between two uniformly accelerated oscillators. *Physical Review D—Particles, Fields, Gravitation, and Cosmology*, 74(8):085031, 2006.

[17] Raphael Bousso. Adventures in de sitter space. *arXiv preprint hep-th/0205177*, 2002.

[18] Marcus Spradlin, Andrew Strominger, and Anastasia Volovich. De sitter space. *Unity from Duality: Gravity, Gauge Theory and Strings: Les Houches Session LXXVI, 30 July–31 August 2001*, pages 423–453, 2002.

[19] Alan H Guth. *The inflationary universe: the quest for a new theory of cosmic origins*. Random House, 1998.

[20] Bruce Allen. Vacuum states in de sitter space. *Physical Review D*, 32(12):3136, 1985.

[21] Bryce S DeWitt. Quantum gravity: the new synthesis. In *General relativity*. 1979.

[22] Björn Garbrecht and Tomislav Prokopec. Unruh response functions for scalar fields in de sitter space. *Classical and Quantum Gravity*, 21(21):4993, 2004.

[23] Hongwei Yu. Open quantum system approach to the gibbons-hawking effect of de sitter space-time. *Physical Review Letters*, 106(6):061101, 2011.

[24] Hongwei Yu and Jialin Zhang. Understanding hawking radiation in the framework of open quantum systems. *Physical Review D—Particles, Fields, Gravitation, and Cosmology*, 77(2):024031, 2008.

[25] Fabio Benatti and R Floreanini. Entanglement generation in uniformly accelerating atoms: Reexamination of the unruh effect. *Physical Review A*, 70(1):012112, 2004.

[26] Jiawei Hu and Hongwei Yu. Entanglement generation outside a schwarzschild black hole and the hawking effect. *Journal of High Energy Physics*, 2011(8):1–13, 2011.

[27] Jun Feng, Yao-Zhong Zhang, Mark D Gould, and Heng Fan. Uncertainty relation in schwarzschild spacetime. *Physics Letters B*, 743:198–204, 2015.

[28] LP Grishchuk and Yu V Sidorov. Squeezed quantum states of relic gravitons and primordial density fluctuations. *Physical Review D*, 42(10):3413, 1990.

[29] Robert H Brandenberger and Jerome Martin. Trans-planckian issues for inflationary cosmology. *Classical and Quantum Gravity*, 30(11):113001, 2013.

[30] Emil Mottola. Particle creation in de sitter space. *Physical Review D*, 31(4):754, 1985.

[31] Andreas Albrecht, Nadia Bolis, and R Holman. Cosmological consequences of initial state entanglement. *Journal of High Energy Physics*, 2014(11):1–18, 2014.

[32] Sugumi Kanno. Cosmological implications of quantum entanglement in the multiverse. *Physics Letters B*, 751:316–320, 2015.

[33] Hael Collins and R Holman. Taming the α -vacuum. *Physical Review D*, 70(8):084019, 2004.

[34] Kevin Goldstein and David A Lowe. A note on α -vacua and interacting field theory in de sitter space. *Nuclear Physics B*, 669(1-2):325–340, 2003.

[35] Martin B Einhorn and Finn Larsen. Interacting quantum field theory in de sitter vacua. *Physical Review D*, 67(2):024001, 2003.

[36] Martin B Einhorn and Finn Larsen. Squeezed states in the de sitter vacuum. *Physical Review D*, 68(6):064002, 2003.

[37] Ulf H Danielsson. On the consistency of de sitter vacua. *Journal of High Energy Physics*, 2002(12):025, 2002.

[38] Jerome Martin and Robert H Brandenberger. Trans-planckian problem of inflationary cosmology. *Physical Review D*, 63(12):123501, 2001.

[39] Nemanja Kaloper, Matthew Kleban, Albion Lawrence, Stephen Shenker, and Leonard Susskind. Initial conditions for inflation. *Journal of High Energy Physics*, 2002(11):037, 2003.

[40] Kevin Goldstein and David A Lowe. Initial state effects on the cosmic microwave background and trans-planckian physics. *Physical Review D*, 67(6):063502, 2003.

[41] Ulf H Danielsson. Inflation, holography, and the choice of vacuum in de sitter space. *Journal of High Energy Physics*, 2002(07):040, 2002.

[42] Ulf H Danielsson. Note on inflation and trans-planckian physics. *Physical Review D*, 66(2):023511, 2002.

[43] Vittorio Giovannetti, Seth Lloyd, and Lorenzo Maccone. Quantum metrology. *Physical review letters*, 96(1):010401, 2006.

[44] Vittorio Giovannetti, Seth Lloyd, and Lorenzo Maccone. Advances in quantum metrology. *Nature photonics*, 5(4):222–229, 2011.

[45] Shunlong Luo. Quantum fisher information and uncertainty relations. *Letters in Mathematical Physics*, 53:243–251, 2000.

[46] Florian Fröwis, Pavel Sekatski, and Wolfgang Dür. Detecting large quantum fisher information with finite measurement precision. *Physical review letters*, 116(9):090801, 2016.

[47] Philipp Hyllus, Wiesław Laskowski, Roland Krischek, Christian Schwemmer, Witlef Wieczorek, Harald Weinfurter, Luca Pezzé, and Augusto Smerzi. Fisher information and multiparticle entanglement. *Physical Review A—Atomic, Molecular, and Optical Physics*, 85(2):022321, 2012.

[48] Sunho Kim, Longsuo Li, Asutosh Kumar, and Junde Wu. Characterizing nonclassical correlations via local quantum fisher information. *Physical Review A*, 97(3):032326, 2018.

[49] Kok Chuan Tan, Seongjeon Choi, Hyukjoon Kwon, and Hyunseok Jeong. Coherence, quantum fisher information, superradiance, and entanglement as interconvertible resources. *Physical Review A*, 97(5):052304, 2018.

[50] Mehdi Ahmadi, David Edward Bruschi, and Ivette Fuentes. Quantum metrology for relativistic quantum fields. *Physical Review D*, 89(6):065028, 2014.

[51] Samira Elghaayda, Asad Ali, Saif Al-Kuwari, and Mostafa Mansour. Physically accessible and inaccessible quantum correlations of dirac fields in schwarzschild spacetime. *Physics Letters A*, 525:129915, 2024.

[52] Yao Yao, Xing Xiao, Li Ge, Xiao-guang Wang, and Chang-pu Sun. Quantum fisher information in noninertial frames. *Physical Review A*, 89(4):042336, 2014.

[53] MY Abd-Rabbou, SI Ali, and N Metwally. Detraction of decoherence that arises from the acceleration process. *JOSA B*, 40(3):585–593, 2023.

[54] Mehdi Ahmadi, David Edward Bruschi, Carlos Sabin, Gerardo Adesso, and Ivette Fuentes. Relativistic quantum metrology: Exploiting relativity to improve quantum measurement technologies. *Scientific reports*, 4(1):4996, 2014.

[55] Mariona Aspachs, Gerardo Adesso, and Ivette Fuentes. Optimal quantum estimation of the unruh-hawking effect. *Physical review letters*, 105(15):151301, 2010.

[56] Danilo Borim, Lucas C Céleri, and Vasileios I Kiosses. Precision in estimating unruh temperature. *arXiv preprint arXiv:2001.09085*, 2020.

[57] Jieci Wang, Zehua Tian, Jiliang Jing, and Heng Fan. Parameter estimation for an expanding universe. *Nuclear Physics B*, 892:390–399, 2015.

[58] David Edward Bruschi, Animesh Datta, Rupert Ursin, Timothy C Ralph, and Ivette Fuentes. Quantum estimation of the schwarzschild spacetime parameters of the earth. *Physical Review D*, 90(12):124001, 2014.

[59] Jun Feng, Xiaoyang Huang, Yao-Zhong Zhang, and Heng Fan. Bell inequalities violation within non-bunch–davies states. *Physics Letters B*, 786:403–409, 2018.

[60] Vittorio Gorini, Andrzej Kossakowski, and Ennackal Chandy George Sudarshan. Completely positive dynamical semigroups of n-level systems. *Journal of Mathematical Physics*, 17(5):821–825, 1976.

[61] Goran Lindblad. On the generators of quantum dynamical semigroups. *Communications in Mathematical Physics*, 48:119–130, 1976.

[62] Fabio Benatti, Roberto Floreanini, and Marco Piani. Environment induced entanglement in markovian dissipative dynamics. *Physical Review Letters*, 91(7):070402, 2003.

[63] Jiawei Hu and Hongwei Yu. Quantum entanglement generation in de sitter spacetime. *Physical Review D*, 88(10):104003, 2013.

[64] Fabio Benatti and R Floreanini. Controlling entanglement generation in external quantum fields. *Journal of Optics B: Quantum and Semiclassical Optics*, 7(10):S429, 2005.

[65] Fabio Benatti, Roberto Floreanini, and Ugo Marzolino. Entangling two unequal atoms through a common bath. *Physical Review A*, 81(1):012105, 2010.

[66] Matteo GA Paris. Quantum estimation for quantum technology. *International Journal of Quantum Information*, 7(supp01):125–137, 2009.

[67] YM Zhang, XW Li, W Yang, and GR Jin. Quantum fisher information of entangled coherent states in the presence of photon loss. *Physical Review A—Atomic, Molecular, and Optical Physics*, 88(4):043832, 2013.

[68] Shunlong Luo. Wigner-yanase skew information and uncertainty relations. *Physical review letters*, 91(18):180403, 2003.

[69] Davide Girolami, Tommaso Tufarelli, and Gerardo Adesso. Characterizing nonclassical correlations via local quantum uncertainty. *Physical review letters*, 110(24):240402, 2013.

[70] Eugene P Wigner and Mutsuo M Yanase. Information contents of distributions. In *Part I: Particles and Fields. Part II: Foundations of Quantum Mechanics*, pages 452–460. Springer, 1997.

[71] Sourav Bhattacharya, Shankhadeep Chakrabortty, and Shivang Goyal. Dirac fermion, cosmological event horizons, and quantum entanglement. *Physical Review D*, 101(8):085016, 2020.

[72] Bruce Allen and Antoine Folacci. Massless minimally coupled scalar field in de sitter space. *Physical Review D*, 35(12):3771, 1987.

[73] Raphael Bousso, Alexander Maloney, and Andrew Strominger. Conformal vacua and entropy in de sitter space. *Physical Review D*, 65(10):104039, 2002.

[74] Juan Maldacena and Guilherme L Pimentel. Entanglement entropy in de sitter space. *Journal of High Energy Physics*, 2013(2):1–31, 2013.

[75] Sugumi Kanno, Jeff Murugan, Jonathan P Shock, and Jiro Soda. Entanglement entropy of α -vacua in de sitter space. *Journal of High Energy Physics*, 2014(7):1–21, 2014.

[76] Amjad Ashoorioon, Konstantinos Dimopoulos, Mohammad M Sheikh-Jabbari, and Gary Shiu. Non-bunch–davis initial state reconciles chaotic models with bicep and planck. *Physics Letters B*, 737:98–102, 2014.